MODELING REMOTE SENSING REFLECTANCE OF HIGHLY TURBID WATERS

J. Wong, S. C. Liew, E. Wong
Centre for Remote Imaging, Sensing and Processing, National University of Singapore
First author contact: crswmcj@nus.edu.sg

1. Introduction

In ocean colour remote sensing, subsurface remote-sensing reflectance (r_{rs}) of water can be linked to its inherent optical properties (IOPs) by various models. The use of such models allow for quick calculations of IOPs from r_{rs} and vice versa, eliminating the need to solve the radiative transfer equation.

In particular, r_{rs} is expressed as a function of a parameter u which is related to the absorption and backscattering coefficients. We note that the quadratic model by Gordon *et al* (*5*) has been widely accepted and validated, at least for case 1 waters. A more recent model by Lee *et al* (*7*) separated the contributions from water and particle scattering. Most models however, only consider oceanic waters where scattering is low. The relationship between r_{rs} and u may deviate from these models in coastal or inland waters with high suspended sediment load.

By running HydroLight (*3*,*4*) simulations in waters with high scattering coefficient values, we found that neither of the models (*5*,*7*) were sufficient to describe the corresponding r_{rs} at high u. A polynomial of *at least* fourth order was required. The non-linear increase may be attributed to multiple scattering by suspended particles in highly turbid waters (*15*). Monte Carlo simulations (*6*) were conducted with similar water types and compared to the results from HydroLight. The Monte Carlo results clearly validated the trend observed from HydroLight simulations.

By incorporating the water-particle separation by Lee *et al* (*7*), we derived a general model relating r_{rs} and IOPs for waters of any turbidity, excluding correction for trans-spectral effects (*9*). The new model is similar to that of Lee *et al* (*7*) at low u, but also accounts for r_{rs} at high u. Application of this derived relationship in relating IOPs to r_{rs} will avoid significant errors in waters of high turbidity.

2. Background

The model by Gordon *et al* (*5*) is

$$r_{rs} = l_1 u + l_2 u^2, \tag{1}$$

where l_1 and l_2 are model parameters, and u is defined as

$$u = \frac{b_b}{a + b_b}, \tag{2}$$

where a is the total absorption coefficient, and b_b is the total backscattering coefficient of the water.

Lee *et al* (*7*) found that it was possible for waters with different a and b_b to have the same u due to water and particle scattering contributions to b_b. They proposed the following model accounting for separate contributions from water and particles

$$r_{rs} = g_w u_w + G_0 u_p \left[1 - G_1 \exp\left(-G_2 u_p\right)\right], \tag{3}$$

where g_w, G_0, G_1, G_2 are model parameters, and

$$u_w = \frac{b_{bw}}{a + b_b}, \tag{4}$$

$$u_p = \frac{b_{bp}}{a + b_b}. \tag{5}$$

The backscattering coefficients b_{bw} and b_{bp} are that of water molecules and suspended particles respectively. It should be noted that the model parameters vary significantly with solar and sensor geometry (*2,13,14*). For the purpose of comparison, we will consider the case of a nadir viewing sensor in this paper. The two models (Eq. 1 and Eq. 3) will be referred to as Gordon88 and Lee04 respectively.

3. Approach

First, we note that variable u lies within the limits $0 < u < 1$ for any type of water. It is thus possible to fully simulate water types over the complete range of u.

a. HydroLight Simulations

We used the HydroLight code (*10,12*) to compute r_{rs} from a wide range of CDOM absorption and particle backscattering coefficients, such that the complete range of u is simulated. The input values used in HydroLight are recorded in Table 1.

The spectral relationships (*1,8*) used to compute the CDOM absorption coefficient $a_g(\lambda)$ and particle backscattering coefficient $b_{bp}(\lambda)$ are

$$a_g(\lambda) = a_g(440) \exp[-S(\lambda - 440)] \tag{6}$$

$$b_{bp}(\lambda) = b_{bp}(550) \left(\frac{550}{\lambda}\right)^{\gamma} \tag{7}$$

The particle scattering phase function was chosen to be a Fournier-Forand phase function (*4*) with $b_{bp}/b_b = 0.018$.

The choice of water component types and wavelengths are of little consequence for the simulations, as the HydroLight code only uses the resulting absorption and backscattering coefficients for its computation.

From the HydroLight output radiance, r_{rs} is calculated with (*2,14*)

$$r_{rs} = \frac{L_u(0^-)}{E_d(0^-)} \tag{8}$$

b. Monte Carlo Simulations

Since HydroLight is *not* commonly used to simulate waters of such high turbidity, a three-dimensional forward Monte Carlo code (*6*) was developed to validate the results for those cases. The Monte Carlo code was run to compute r_{rs} with the same input parameters as HydroLight (Table 1). Upon reaching the water surface, the photons were consolidated by 240 solid angle 'quads', exactly as defined in the HydroLight program (*10*), so that the results can be compared.

The incident radiation field was defined by using the subsurface downwelling radiance, $L_d(0^-)$ from the output of a sample HydroLight run. For each set of IOP combination, approximately 10^6 photons were initiated per wavelength, with the number of photons per direction scaled by the normalised $L_d(0^-)$ field.

In the Monte Carlo program, the r_{rs} is computed by (*6*)

$$r_{rs} = \frac{1}{\mathrm{N} \cdot \Omega} \sum_{i=1}^{n} \frac{1}{|cos\theta_i|} \tag{9}$$

where N is the number of downwelling photons, Ω is the solid angle of the quad containing the exit direction, n is the number of upwelling photons reaching the surface, and θ_i is the exit zenith angle of the i-th photon reaching the surface.

4. Results

The r_{rs} computed from HydroLight is plotted against u in Figure 1, together with the Gordon88 and Lee04 models. The Lee04 model is not dependent on a single variable u, so we plot only the particle contribution against u_p. The water contribution in Lee04 is negligible in our region of interest (turbid waters).

In Figure 1, the r_{rs} from HydroLight simulations increases faster with u when u is large compared with the Gordon88 and Lee04 models. It diverges from Gordon88 at $u \approx 0.3$, and from Lee04 at $u \approx 0.7$. The increasing trend is clearly greater then linear, possibly due to the multiple scattering of photons on the suspended particles (*15*). From Eq. 3, the Lee04 model behaves linearly at high u, and is unable to account for the increased r_{rs}. While Gordon88 is a quadratic function of u, its increase is not fast enough to match the increase in r_{rs} at high u.

To make a meaningful quantitative comparison between the HydroLight data and the models, we divide u into 3 ranges of low, mid, and high u. The boundaries of these ranges are $u = 0.4$ and $u = 0.8$, near the points where the two models diverge significantly from the HydroLight results. The average percentage difference (APD) is then calculated[1]. As expected, both models do well in low u ($APD < 10\%$). In mid u, Gordon88 has an APD of 16.9%, and Lee04, 2.6%. In high u, Gordon88 has an APD of 23.1%, and Lee04, 13.8%.

The APD at saturation ($u > 0.95$) was computed to show the maximum error at the highest turbidity levels. The maximum APDs were found to be 30.2% and 24.1% for Gordon88 and Lee04 respectively. The APDs between HydroLight and each of the models are summarised in Table 2.

To validate the HydroLight simulation results at high u, Monte Carlo simulations were run with similarly randomised IOPs. The Monte Carlo results for nadir-viewing r_{rs} is plotted in Figure 1. The relationship between r_{rs} and u from the Monte Carlo simulations follow a similar trend, resembling that of HydroLight. Like the previous observation, the rate of increase of r_{rs} is larger than both established models at high u.

[1] For Lee04, the APD was calculated with the full model, *i.e.* with both water and particle terms.

5. Modelling r_{rs} in High Turbidity

Results from both HydroLight and Monte Carlo suggest that the r_{rs} dependence on u is greater than the 2nd power. For the sake of reproducibility, we used the HydroLight results to develop the subsequent model. By doing a rough fit of the HydroLight data to various curves, we found that polynomials of 4th, 6th, and 8th order fit the points well. The 4th order polynomial fits most of the points up to $u \approx 0.95$ where it diverges from the trend, while the 6th order polynomial fits the points at high u better.

The APD of the three polynomials with HydroLight are calculated and presented in Table 2. While the lowest APDs lie in the 6th and 8th order polynomial fitting, the APDs of the 4th order polynomial are already smaller than the uncertainty associated with r_{rs} or IOP measurements. As such, we choose to use the 4th order polynomial to model r_{rs} at high u.

6. Development of a General Model

A previous model by Park & Ruddick (*14*) expressed the above-water remote sensing reflectance (R_{rs}) as a 4th order polynomial of u. However, their model coefficients were a function of b_{bp}/b_b in addition to the sun-sensor geometry, to account for differences in the rate of increase of R_{rs} with u. Their HydroLight simulations of water types extended only up to $u = 0.5$. For practical usage, we aim to develop a model which is applicable across the whole range of u, with coefficients depending only on the sun-sensor geometry.

In the development of our general model that extends to high turbidity, a main consideration was to be able to reproduce the results of existing established models at low turbidity. In particular, the Lee04 model accounted for multiple g values (i.e. the ratio r_{rs}/u) from the same u due to the different shapes of the water molecule and particle volume scattering functions (*7*). This effect is more significant at low u. A close fit is especially important in that range, since even a small deviation in r_{rs} would result in large percentage errors.

The HydroLight results (1,167,296 points per sun-sensor geometry set) were fitted to the following model

$$r_{rs} = g_w u_w + \sum_{i=1}^{4} g_i u_p^i \,, \tag{10}$$

where g_w, g_i are the model parameters dependent on the sun-sensor geometry.

To ensure that the error at low u is not amplified by the imperfect fit of the quartic polynomial, the HydroLight generated r_{rs} was initially fitted to the model in the low u region to determine values of g_w. Fixing g_w, a second fitting of HydroLight r_{rs} to the model was performed for all data points to obtain the coefficients $g_i (i = 1,2,3,4)$ by minimising the absolute difference weighted by $\left(1 - u_p\right)^2$. The following relation was obtained for nadir-viewing sensors

$$r_{rs} = 0.099\, u_w + 0.072\, u_p + 0.296\, u_p^2 - 0.363\, u_p^3 + 0.240\, u_p^4. \tag{11}$$

The model is plotted against u in Figure 2 with the HydroLight results, and the resulting APDs are listed in Table 2. The r_{rs} of HydroLight simulations versus the new quartic model is presented in Figure 3. As intended, the APDs are small from the low to high u range, and does

not exceed 5% in the saturation range. Examining the errors of all the points from Eq. 11, we found an average error of 0.3% and a maximum error of 7.6%.

In Table 3, we have listed the coefficients for commonly used sensor geometries (*2*,*11*,*12*).

7. Conclusion

From the results of the HydroLight and Monte Carlo simulations, it is determined that r_{rs} has at least a quartic dependence on u, possibly due to multiple scattering by particles. The HydroLight data points were fit to a quartic polynomial model, which included a term for water contribution based on the Lee04 model. From the fitting to this new quartic model, an average error of 0.3% and maximum error of 7.6% was found. This model is thus better suited to waters of high turbidity. In the event that higher accuracy in the saturation range is required, new coefficients can be derived from HydroLight simulations in that range of u, or by a different choice of weight in fitting HydroLight data to Eq. 10.

Acknowledgements

The authors acknowledge funding support from Office for Space Technology and Industry, Singapore (Project Reference: S15-1320-NRF-OSTIn-SRP). We are also grateful to ZhongPing Lee for his comments and suggestions.

References

1. A. Bricaud, A. Morel, and L. Prieur, Absorption by dissolved organic matter of the sea (yellow substance) in the UV and visible domains'. *Limnol. Ocean.* **26,** pp. 43–53 (1981).

2. K. P. Du, Z. P. Lee, M. X. He, Z. S. Liu, K. L. Carder, and F. Zhao, Angular variation of remote-sensing reflectance and the influence of particle phase functions, paper presented at *IGARSS 2004: IEEE International Geoscience and Remote Sensing Symposium Proceedings*, pp. 845–848

3. B. Fougnie, R. Frouin, and P. Deschamps, Reduction of skylight reflection effects in the above-water measurement of diffuse marine reflectance. *Appl. Opt.* **39,** pp. 3844–3856 (2000).

4. G. R. Fournier and J. L. Forand, Analytic phase function for ocean water, paper presented at *Ocean Optics XII*, pp. 194–201

5. H. R. Gordon, O. B. Brown, R. H. Evans, J. W. Brown, R. C. Smith, K. S. Baker, and D. K. Clark, A Semianalytic Radiance Model of Ocean Color. *J. Geophys. Res.* **93,** pp. 10909–10924 (1988).

6. R. A. Leathers, T. V. Downes, O. D. Curtiss, and C. D. Mobley, *Monte Carlo Radiative Transfer Simulations for Ocean Optics: A Practical Guide*. (2004).

7. Z. Lee, K. L. Carder, and K. Du, Effects of molecular and particle scatterings on the model parameter for remote-sensing reflectance. *Appl. Opt.* **43,** pp. 4957–4964 (2004).

8. Z. Lee, K. L. Carder, C. D. Mobley, R. G. Steward, and J. S. Patch, Hyperspectral remote sensing for shallow waters: 2 Deriving bottom depths and water properties by optimization. *Appl. Opt.* **38,** pp. 3831–3843 (1999).

9. Z. Lee and Y. Huot, On the non-closure of particle backscattering coefficient in oligotrophic oceans. *Opt. Express* **22,** p. 29,223-29,233 (2014).

10. C. D. Mobley, *Hydrolight 3.0 User's Guide*. (1995).

11. C. D. Mobley, Estimation of the remote-sensing reflectance from above-surface measurements. *Appl. Opt.* **38,** pp. 7442–7455 (1999).

12. C. D. Mobley, Light and Water: Radiative transfer in the natural waters. (1994).

13. A. Morel and B. Gentili, Diffuse reflectance of oceanic waters. II. Bidirectional aspects. *Appl. Opt.* **32,** pp. 6864–6879 (1993).

14. Y.-J. Park and K. Ruddick, Model of remote-sensing reflectance including bidirectional effects for case 1 and case 2 waters. *Appl. Opt.* **44,** p. 1236 (2005).

15. M. Sydor, R. W. Gould, R. A. Arnone, V. I. Haltrin, and W. Goode, Uniqueness in remote sensing of the inherent optical properties of ocean water. *Appl. Opt.* **43,** pp. 2156–2162 (2004).

16. J. R. V. Zaneveld and V. Z. J. Ronald, A theoretical derivation of the dependence of the remotely sensed reflectance of the ocean on the inherent optical properties. *J. Geophys. Res.* **100,** p. 13,135-13,142 (1995).

Tables and Figures

Table 1: Input parameters used in HydroLight and Monte Carlo simulations.

HydroLight/Monte Carlo Parameter	**Input/Values**
Solar zenith angle	30°
Wavelength (nm)	$400 - 700$, every $5nm$
$a_g(440)$	Randomised between $0.03 - 2\ m^{-1}$
S	Randomised between $0.01 - 0.02$
$b_{bp}(550)$	Randomised between $0.03 - 1\ m^{-1}$
γ	Randomised between $0 - 1.2$
Particle scattering phase function	Fournier-Forand, $b_{bp}/b_p = 0.018$
Water depth	Infinitely Deep

Table 2: Average percentage difference between HydroLight results, and the specified model.

Model	**Low u** $\mathbf{0.0 < u \leq 0.4}$	**Mid u** $\mathbf{0.4 < u \leq 0.8}$	**High u** $\mathbf{0.8 < u < 1.0}$	**Saturation** $\mathbf{0.95 < u < 1.0}$
Gordon88	9.4	16.9	23.1	30.2
Lee04	2.3	2.6	13.8	24.1
4th Deg Poly	2.7	0.4	0.8	1.6
6th Deg Poly	1.2	0.3	0.4	0.6
8th Deg Poly	0.7	1.1	2.8	4.1
New Quartic	0.5	0.2	0.7	4.7

Table 3: Model coefficients for the new quartic model, with $\theta_{sun} = 30°$.

Sensor Geometry	$\boldsymbol{g_w}$	$\boldsymbol{g_1}$	$\boldsymbol{g_2}$	$\boldsymbol{g_3}$	$\boldsymbol{g_4}$
Nadir	0.099	0.073	0.296	-0.363	0.240
$\theta = 20°, \phi = 90°$	0.100	0.074	0.304	-0.382	0.250
$\theta = 40°, \phi = 90°$	0.103	0.079	0.319	-0.424	0.272
$\theta = 40°, \phi = 135°$	0.092	0.082	0.335	-0.461	0.294

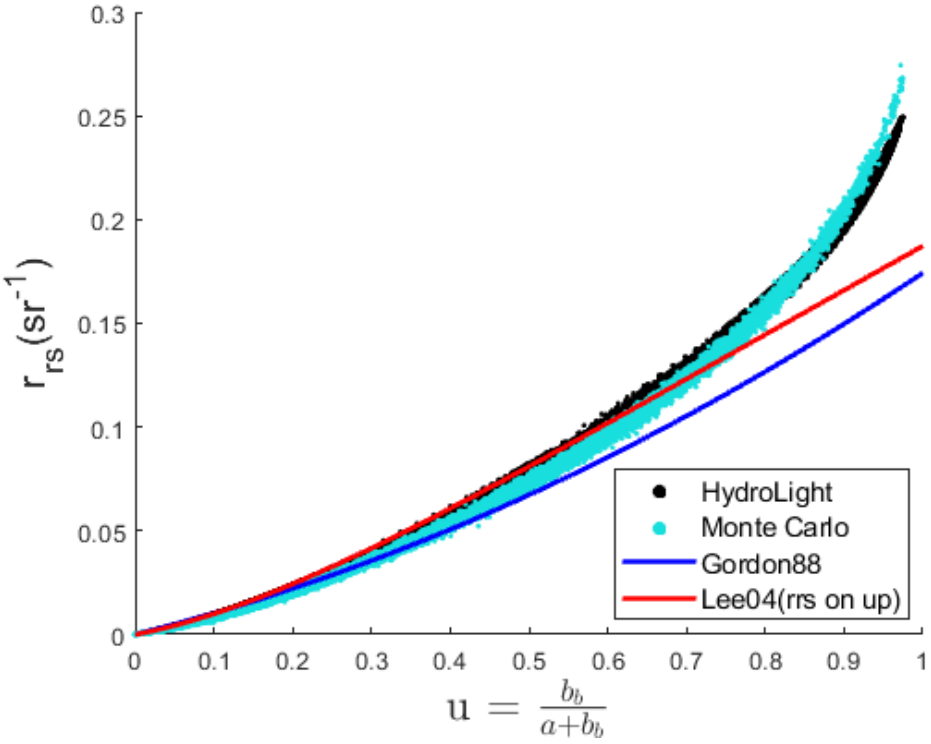

Figure 1: Scatter plot of r_{rs} on u from the HydroLight and Monte Carlo simulations. For comparison, the Gordon88 model is plotted, as well as the particle term from Lee04. The r_{rs} is taken at nadir.

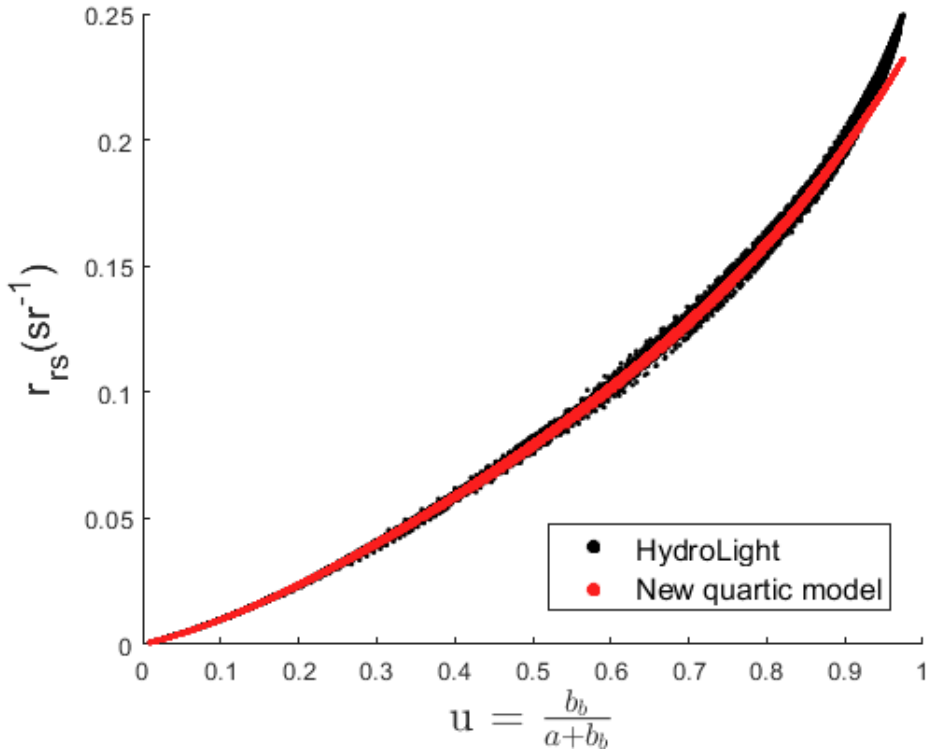

Figure 2: Scatter plot of r_{rs} on u, of the new quartic polynomial model (on HydroLight u) and HydroLight results.

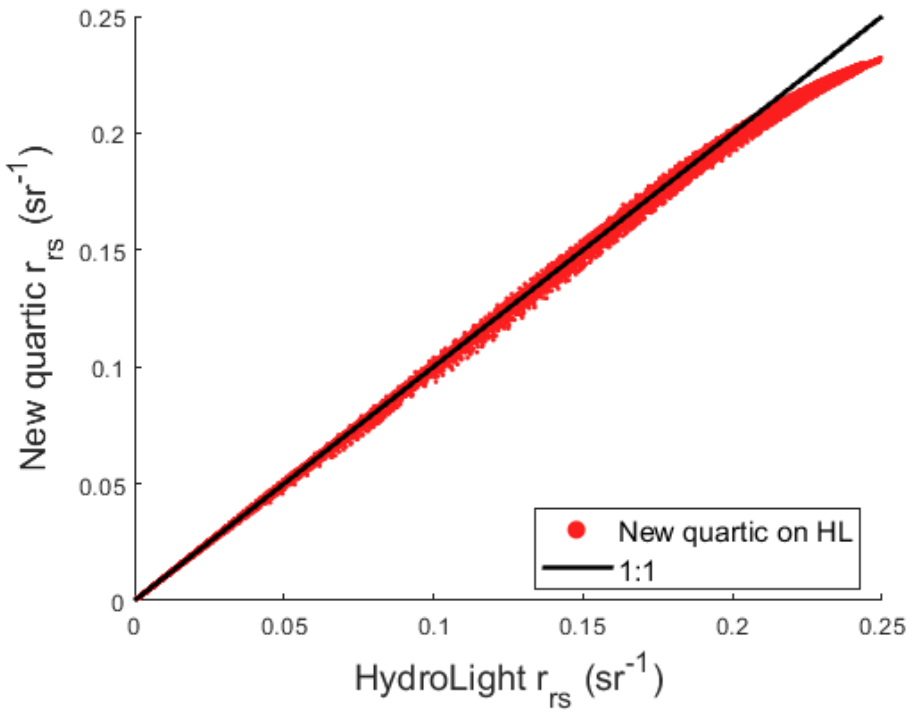

Figure 3: r_{rs} values of the new quartic model compared with r_{rs} values from HydroLight.